DOI: 10.1002/chem.200500021

Pulsed Gradient Spin Echo (PGSE) Diffusion Measurements as a Tool for the Elucidation of a New Type of Hydrogen-Bonded Bicapsular Aggregate

Mateo Alajarín,*[a] Aurelia Pastor,*[a] Raúl-Angel Orenes,[a] Eloísa Martínez-Viviente,[b] and Paul S. Pregosin[b]

Abstract: Compounds formed by linking two tris(ureidobenzyl)amine modules with a hexamethylene tether are described. These compounds self-assemble to form bicapsular aggregates featuring two rings of six hydrogen-bonded ureas. ^{1}H and ^{1}H/^{1}H ROESY NMR spectroscopy, together with pulsed gradient spin echo (PGSE) NMR diffusion measurements, have been used to characterize the dimers in solution. The results have been compared with energy-minimized structures. The new compounds are kinetically stable on the NMR timescale, and their thermodynamic stabilities are comparable to other capsular aggregates derived from tris(ureidobenzyl)-amines.

Keywords: diffusion · hydrogen bonds · NMR spectroscopy · self-assembly · structure elucidation

Introduction

Multiple hydrogen-bond formation has opened the door to a useful approach for assembling individual molecular components into functional organic nanostructures that are held together in a reversible manner.[1] Molecules containing the correct structural information spontaneously assemble into helices,[2] rosettes,[3] cylinders,[4] capsules,[5] dendrimers,[6] polymers,[7] or grids.[8] Urea functionalities have a great tendency to form hydrogen bonds, not only in the solid state, but also in solution.[9] Recently, some of us have proved that the triureas **1**, derived from the tribenzylamine skeleton, assemble to form dimeric aggregates (Scheme 1).[10] In these dimers two molecules associate by forming hydrogen bonds between the six ureas, forming a head-to-tail directional array of 12 hydrogen bonds.[10] The result is a capsular aggregate with an internal cavity, that is too small for the encapsulation of organic molecules.[10a,c]

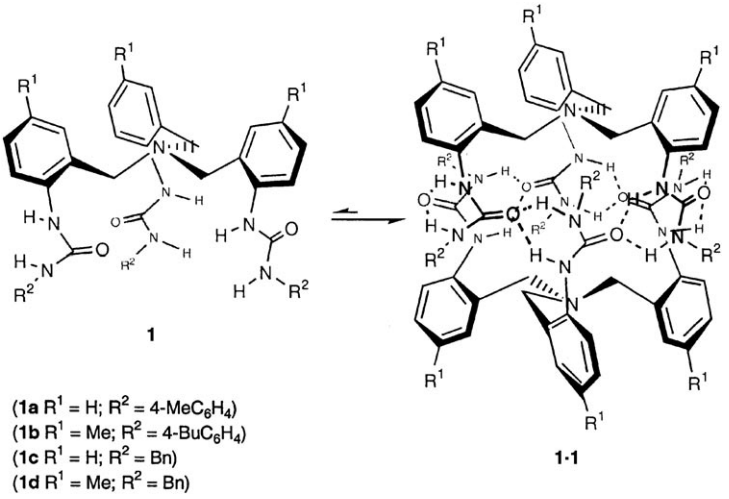

Scheme 1. Tris(2-ureidobenzyl)amines **1** dimerize in the solid state and in solution to form capsular aggregates.

Unimolecular capsules could in principle be achieved from a molecule containing two tripodal subunits of tris(ureidobenzyl)amine, linked through their urea residues by means of a flexible tether. This spacer should be long enough to allow the folding of the molecule to form the ring of hydrogen-bonded ureas, but short enough to minimize the increase in entropy brought about by the freely rotating single bonds. A hexamethylene spacer has previously been

[a] Prof. Dr. M. Alajarín, Dr. A. Pastor, R.-A. Orenes
Departamento de Química Orgánica
Facultad de Química, Universidad de Murcia
Campus de Espinardo, Murcia-30.100 (Spain)
Fax: (+34) 968-364-149
E-mail: alajarin@um.es
aureliap@um.es

[b] Dr. E. Martínez-Viviente, Prof. Dr. P. S. Pregosin
Laboratory of Inorganic Chemistry
ETHZ, Hönggerberg, 8093 Zürich (Schweiz)

Supporting information for this article is available on the WWW under http://www.chemeurj.org/ or from the author. It contains a ^{1}H/^{1}H ROESY spectrum of the triurea **1a** ($CDCl_3$), as well as energy-minimized structures of compounds **2b·2b** and **6**.

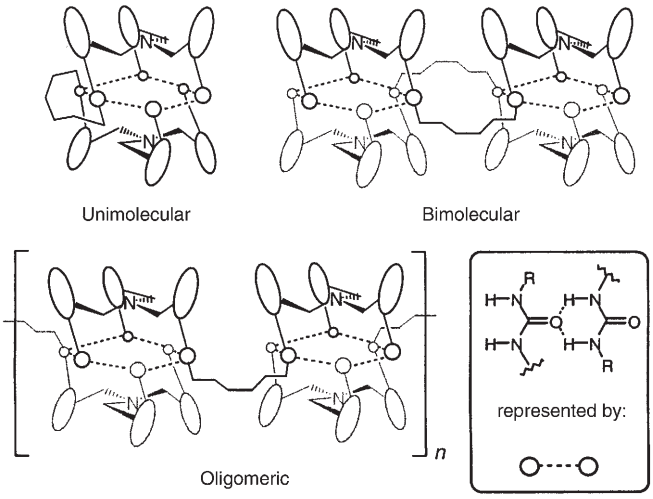

Figure 1. Schematic representation of the self-assembly of **2** to yield unimolecular, bimolecular, or oligomeric aggregates.

used to successfully link two tetraureidocalixarenes, leading to unimolecular capsules.[11] Consequently, we decided to introduce this structural fragment into our tris(ureidobenzyl)amine system. In principle, such a modified structure would allow several types of assembly to occur (Figure 1), such as: 1) intramolecular self-assembly to give a unimolecular capsule, 2) intermolecular assembly to give a bimolecular species, and 3) oligomerization to higher order systems.

Whereas, examples of assembly by hydrogen bonding to afford unimolecular[11,12] or polymeric capsules[7c–e] are well-known in the literature, bicapsular aggregates assembled exclusively by hydrogen bonding are rare. Rebek[7c,11] has reported an example based on a heterotrimer. Cram,[13] Sherman,[14] Nolte,[15] and Liu[16] have reported several bicapsules based on the highly restricted resorcarene skeleton and on two metallobridged bis(β-CyDs) complexes, but these capsules were formed by covalent synthesis, and not exclusively by hydrogen-bond assembly.

The characterization of assembling systems in solution often relies on a combination of NMR spectroscopy, mass spectrometry, vapor pressure osmometry (VPO), and gel permeation chromatography (GPC). However, as the molecules increase in complexity, new analytical tools are required.[17] Recently, pulsed gradient spin echo (PGSE) NMR diffusion measurements[18] have proved to be a useful tool for probing encapsulation and studying the structure of hydrogen-bonded capsules in solution.[19] The diffusion coefficient (D) depends on the molecular shape and size (the larger the molecule, the lower the D value). Thus, it should be possible to distinguish between the unimolecular, bimolecular, and oligomeric species in Figure 1 on the basis of their diffusion coefficients. We present here our PGSE diffusion measurements on the hexaureas **2a**,**b** (Scheme 2) and related species. These results, together with ^{1}H NMR and 2D NOE spectroscopic data, provide conclusive evidence of the solution structures of these systems.

Results and Discussion

Synthesis: The synthetic procedure leading to the hexaureas **2a,b** is shown in Scheme 2. The key intermediate **3** was prepared in 93% yield by the reaction of 2-azidobenzylamine with 2-nitrobenzyl iodide in the presence of Na_2CO_3. The formation of the corresponding iminophosphorane by the reaction of **3** with trimethylphosphine, followed by hydrolysis in THF/H_2O, gave the amine **4** (67–90%). After reaction with 1,6-diisocyanatohexane, the bis(tribenzylamine) derivative **5** was isolated in 69% yield. Finally, the hexaureas **2** were obtained from **5** by the following two-step sequence. First, catalytic hydrogenation of **5** afforded the tetraamino intermediate **6** in 91% yield. Second, this intermediate was

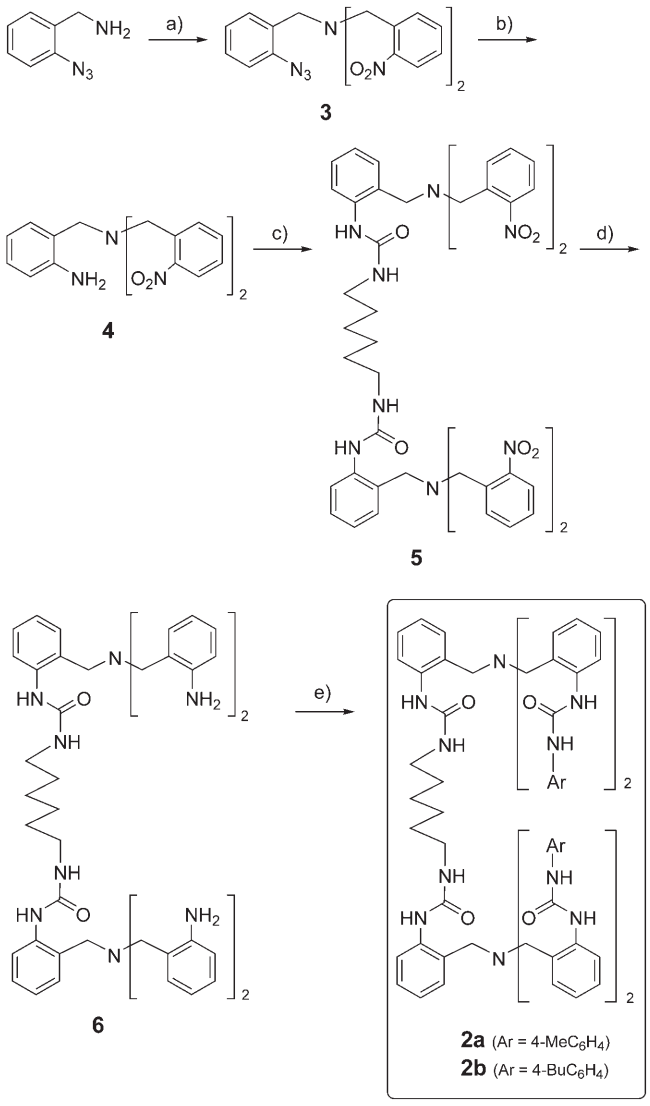

Scheme 2. Reagents and reaction conditions for the synthesis of the hexaureas **2a**,**b**: a) 2-nitrobenzyl iodide, Na_2CO_3, MeCN, reflux, 24 h. b) i) PMe_3, THF, 0°C, 30 min. ii) THF/H_2O, 20°C, 20 h. c) OCN-$(CH_2)_6$NCO, $CHCl_3$, 100°C, 30 h. d) H_2, PtO_2, THF, 20°C, 20 h. e) ArNCO, $CHCl_3$, reflux, 24 h.

reacted with the corresponding aryl isocyanate to give **2a,b** in 58–60% yield.

^{1}H NMR spectroscopy: Figure 2 shows ^{1}H NMR spectra for solutions of **1a** and **2a** in [D_6]DMSO and $CDCl_3$. In a strongly hydrogen-bonding solvent, such as [D_6]DMSO, **1a** and **2a** exist as monomeric, nonassembled species. For **2a** (Figure 2b), the two types of benzylic methylene groups appear as two singlets at $\delta = 3.56$ and 3.59 ppm. The *p*-tolyl methyl groups give a singlet at $\delta = 2.21$ ppm, and the aromatic protons of the pendant *p*-tolyl groups afford the usual AA′XX′ pseudodoublets in the region of $\delta = 7.00$–7.30 ppm. These chemical shifts for **2a** are similar to those found for **1a** in [D_6]DMSO (Figure 2a).[10a,c]

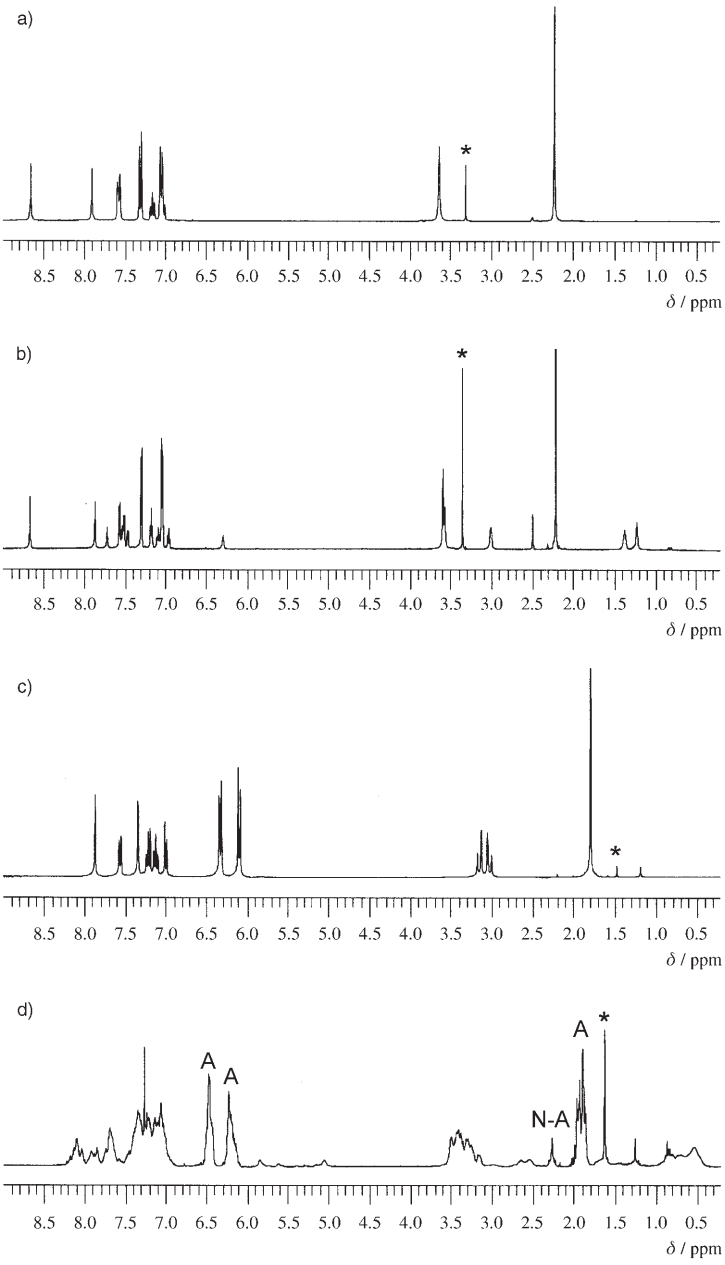

Figure 2. ^{1}H NMR spectra (300 and 600 MHz) of 0.020 M solutions of a) **1a** in [D_6]DMSO, b) **2a** in [D_6]DMSO, c) **1a** in $CDCl_3$, and d) **2a** in $CDCl_3$. **A** and **N-A** mark the resonances exclusively due to assembled and nonassembled species, respectively. The asterisk labels the signal for residual water.

The change to a noncompetitive solvent, such as $CDCl_3$, produces significant alterations in the solution structures of **1a** and **2a**, as indicated by the ^{1}H NMR spectra (Figure 2c and d). As mentioned in the introduction, the triurea **1a** has been previously investigated.[10a,c] A combination of techniques (X-ray analysis, NMR and IR spectroscopy, and ESI-MS) provided evidence for a dimeric, capsular structure **1a·1a**, both in the solid-state and in $CDCl_3$.[10a,c] Three aspects of that research are of relevance for the present discussion: 1) When **1a** is dissolved in $CDCl_3$, the ^{1}H NMR spectrum (Figure 2c) shows a loss of symmetry with respect to the spectrum in [D_6]DMSO (Figure 2a). 2) The resonances of the aromatic and methyl protons of the *p*-tolyl groups in $CDCl_3$, are shifted to lower frequencies with respect to those in [D_6]DMSO. This effect can be attributed to local anisotropic effects within the capsule **1a·1a**.[10a,c] 3) The ROESY spectrum in $CDCl_3$ (see Supporting Information, Figure S.1[10c]) shows NOE contacts between the aromatic and methylenic protons of the tribenzylamine moiety and the aromatic protons of the *p*-tolyl groups.[10c] As shown in Figure S.1,[10c] these contacts nicely support the formation of a capsular dimeric aggregate **1a·1a**, as they are difficult to explain in a monomeric **1a**.[10c] Indeed, these NOE contacts are not present in the ROESY spectrum of **1a** in [D_6]DMSO, in which the compound exists as a nonassembled monomer.[10c]

Although compound **2a** was purified by chromatography (EtOAc/hexane 1:3), and was thus expected to be a single species, the ^{1}H NMR spectrum of **2a** in $CDCl_3$ is poorly resolved and shows a mixture of different species (Figure 2d). By a comparison of this spectrum with that of **1a·1a** in $CDCl_3$ (see Figure 2c and the previous paragraph), the broad resonances at approximately $\delta = 1.90$, 6.20, and 6.50 ppm can be assigned to the methyl and aromatic protons of the *p*-tolyl groups in a capsular derivative of **2a**. As shown in Figure 1, this derivative could, in principle, be a self-assembled monomer, a dimer, or an oligomer. Other signals in this spectrum might belong to a nonassembled monomeric species, for example, the peak at $\delta = 2.26$ ppm is in agreement with the methyl signal observed for **2a** in [D_6]DMSO, in which this compound is a nonassembled monomer. All the resonances in $CDCl_3$ are broad and complex, pointing to a distribution of isomers, both for the assembled and nonassembled species. Figure 3 shows a comparison between the methyl region from the ^{1}H NMR spectrum of **2a** in $CDCl_3$ at 2×10^{-3} M (Figure 3a, 700 MHz) and at 0.020 M (Figure 3b, 600 MHz, expansion from Figure 2d). At the lower concentration, the nonassembled species (indicated by the higher resonance frequencies) are predominant. We will return to the ^{1}H NMR spectrum of **2a** in a later discussion of the NOEs.

The ^{1}H NMR spectra of **2b** (which contains an *n*-butyl instead of a methyl substituent) in [D_6]DMSO and $CDCl_3$ are

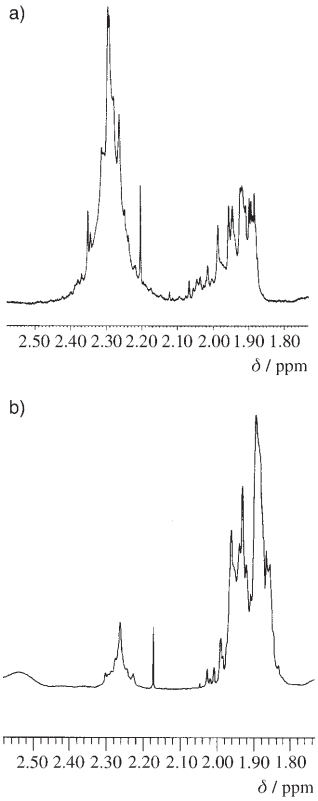

Figure 3. Methyl region of the ^{1}H NMR spectrum of **2a** in a) $CDCl_3$ (2×10^{-3} M), measured at 700 MHz and b) $CDCl_3$ (0.020 M), measured at 600 MHz. The complexity and line width of the signals suggest several isomers of both species, that is assembled and nonassembled.

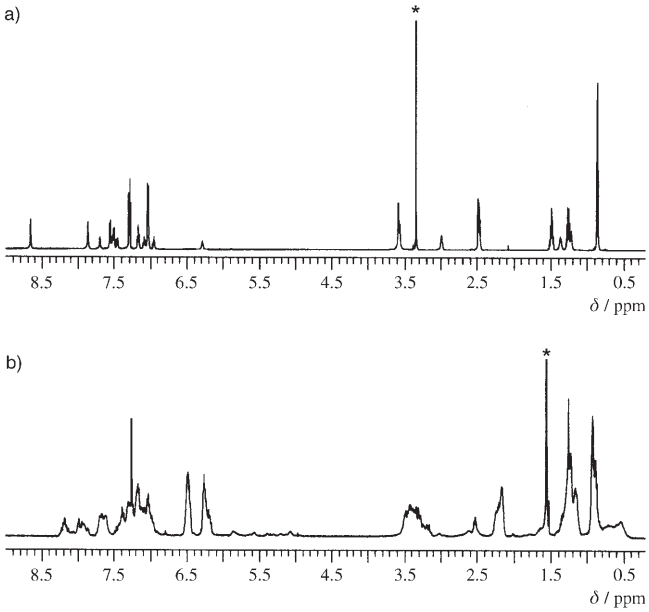

Figure 4. ^{1}H NMR spectrum of a) **2b** in [D_6]DMSO (0.020 M, 600 MHz) and b) **2b** in $CDCl_3$ (1×10^{-3} M, 500 MHz). The asterisk labels the signal for residual water.

shown in Figure 4. Based on the anisotropy criterion mentioned above, the multiplets between $\delta=6.10$ and 6.60 ppm correspond to the aromatic protons of the *p*-BuC_6H_4 groups in an assembled species (monomer, dimer, or oligomer). At first sight, it is not clear whether nonassembled, monomeric **2b** is also present in this solution. However, since the intensity of the weak resonance at $\delta=2.5$ ppm increases with added DMSO, we suggest that this weak signal might correspond to the butyl CH_2 group in nonassembled **2b** (see below for further discussion).

Clearly, although the proton spectra for **2a** and **2b** in $CDCl_3$ are informative, the nature of the aggregates remains uncertain.

PGSE measurements: To estimate the molecular volumes (and thus the aggregation states) of the two different species present in $CDCl_3$, we have carried out PGSE diffusion measurements on solutions of **2a** and **2b** in $CDCl_3$. Solutions of the triurea **1a** and the precursor **6** in $CDCl_3$ (shown in Scheme 2) were also studied (Table 1 and Figure 5). Table 1 includes the calculated hydrodynamic radii, obtained from the *D* values by the Stokes–Einstein equation.[20] The chemical shifts of the peaks used in the determination of the *D* values are indicated in the Table.

The ratio between the *D* values for the assembled and nonassembled species in **2a** is 4.28/3.31 = 1.29. For spherical molecules, this number corresponds to a mass ratio of approximately 2:1.[17b,21] As the nonassembled molecules must be monomers, a dimeric structure is proposed for the aggregates. We do not find polymers of **2a** in $CDCl_3$, at least not at measurable concentrations. The PGSE measurements on the aromatic region ($\delta=7.0$–7.3 ppm) of this mixture **2a**/**2a·2a** afford a *D* value (4.11×10^{-10} m^{2}s^{-1}) that is only slightly smaller than the value assigned to the monomer (4.28×10^{-10} m^{2}s^{-1}, Table 1). Indeed, in this aromatic region the most intense signals are expected to stem from the *p*-tolyl protons of the monomer, which at 2×10^{-3} M represents the predominant species (ratio **2a**:**2a·2a** 1:0.4, Figure 3a).

For the solution of **2b** in $CDCl_3$, the *D* value measured using the resonances at $\delta=6.5$ ppm (3.16×10^{-10} m^{2}s^{-1}, Table 1) is similar to that found for **2a·2a** (3.31×10^{-10} m^{2}s^{-1}), confirming the assignment of these signals to the dimeric species **2b·2b**. The substitution of Me in **2a·2a** with *n*Bu in **2b·2b** produces the expected modest decrease

Table 1. Diffusion coefficients (*D* [m^{2}s^{-1}]) and hydrodynamic radii (r_H [Å]) of **1a**, **2a**, **2b**, and **6** in $CDCl_3$ (2×10^{-3} M) at 299 K.[a]

		δ [ppm]	$D^{[b]}\times10^{-10}$	r_H[c]
1a	assembled (**1a·1a**)	1.89, 7.43, 7.96	5.24	7.8
2a	assembled (**2a·2a**)	1.93, 6.22, 6.46	3.31	12.4
	nonassembled (monomer)	2.26	4.28	9.6
	mixture	7.0–7.3	4.11[d]	–
2b	assembled (**2b·2b**)	6.5	3.16	13.0
	nonassembled (monomer)	2.5	4.04	10.1
6	precursor	6.61, 6.73	5.76	7.1

[a] $\eta=0.534\times10^{-3}$ Kg s^{-1} m^{-1} ($CDCl_3$, 299 K). [b] Experimental error is approximately ±2%. [c] Standard deviation is approximately ±0.1 Å. [d] Average of values for $\delta=7.06$ (4.08×10^{-10} m^{2}s^{-1}), 7.19 (4.19×10^{-10} m^{2}s^{-1}), and 7.22 ppm (4.06×10^{-10} m^{2}s^{-1}).

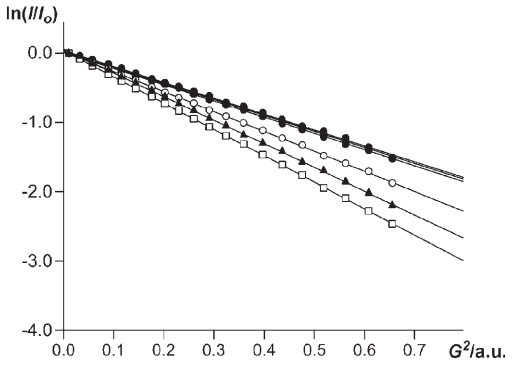

Figure 5. Plot of $\ln(I/I_o)$ versus arbitrary units proportional to the square of the gradient amplitude for ^{1}H PGSE diffusion measurements on solutions of **2a** (circles), **1a** (triangles), and **6** (squares) in $CDCl_3$ (2×10^{-3} M). For **2a**, the full circles correspond to the measurements on the signals of the dimer ($\delta=1.93$, 6.22, and 6.46 ppm) and the open circles correspond to the measurements on the signals of the monomer at $\delta=2.26$ ppm. For **1a**, all of the compound is present as a dimer at this concentration. The NMR spectroscopic parameters are the same for all of the reproduced measurements ($\Delta=93$ ms, $\delta=1.75$ ms, 16 scans, for an explanation see Experimental Section).

in D. For the weak resonance at $\delta=2.5$ ppm, $D=4.04\times10^{-10}$ m^{2}s^{-1} and $r_H=10.1$ Å support the tentative assignment of this resonance to the monomer. Other signals from the spectrum of **2b** in $CDCl_3$ afforded intermediate D values, presumably, due to an overlap of the peaks produced by the monomer and dimer.

The triurea **1a** exists only as the dimer **1a·1a** in $CDCl_3$ at the concentration studied. The hydrodynamic radius of the monomer of **2a** (9.6 Å) is larger than for **1a·1a** (7.8 Å), although the structures of these compounds seem at first sight to be similar. The difference in size may be explained by the presence of the tether linking group in **2a**, as well as by a more compact, assembled structure in **1a·1a**. The precursor **6** is the smallest molecule shown in Table 1, although it is almost as large as the compact assembly **1a·1a**. As the "smallest" compound, **6** reveals the larger slope in Figure 5.

In [D$_6$]DMSO, **1a** and **2a** exist as monomeric, nonassembled species (Table 2). As a result of the higher viscosity of this solvent, all the D values in [D$_6$]DMSO are considerably smaller than in $CDCl_3$. However, as the calculated r_H values are viscosity-corrected,[20] they allow for a comparison of the PGSE results for both solvents. For **6**, the aggregation state of which does not change with the solvent, the r_H value in [D$_6$]DMSO is 1 Å larger than in $CDCl_3$, and we attribute this difference to solvation and/or hydrogen bonding by the [D$_6$]DMSO solvent. Since the solvation should be at least as strong for **1a**, **2a**, and **2b** as for **6**, we have made a crude empirical correction of -1 Å for all of the r_H values obtained in [D$_6$]DMSO. The resulting radii (r_c in Table 2) are the suggested upper limits for the molecular radii of the species present in [D$_6$]DMSO. These r_C values for **2a** and **2b** are similar to the r_H values obtained for the monomers of these species in $CDCl_3$ (also shown in Table 2).

Table 2. Diffusion coefficients (D [m^{2}s^{-1}]) and hydrodynamic radii (r_H [Å]) of **1a**, **2a**, **2b**, and **6** in [D$_6$]DMSO (2×10^{-3} M) at 299 K. The r_H values for the monomers in $CDCl_3$ are given for comparison.[a]

	$D^{[b]}\times10^{-10}$	r_H[c]	r_C[d]	r_H[c] (monomer, $CDCl_3$)
1a	1.51	7.5	6.5	–[e]
2a	1.05	10.7	9.7	9.6
2b	1.03	11.0	10.0	10.1
6	1.40	8.1	7.1	7.1

[a] $\eta=1.940\times10^{-3}$ Kg s^{-1} m^{-1} ([D$_6$]DMSO, 299 K). [b] Experimental error is approximately ±2%. [c] Standard deviation is approximately ±0.1 Å. [d] Corrected for [D$_6$]DMSO solvation. [e] For **1a** in $CDCl_3$ there was no monomer present.

We were curious to know if the average D value of the solvent [D$_6$]DMSO would be affected by the presence of **1a**, **2a**, **2b**, or **6** in the solution, due to hydrogen bonding with the solute. Table 3 shows the D values of a reference sample of DMSO, plus the D values of the solvent in the solutions studied. Not surprisingly, in these relatively dilute solutions (2×10^{-3} M), such an effect was not observed.

Table 3. Diffusion coefficients (D [m^{2}s^{-1}]) for the residual protonated solvent in solutions of **1a**, **2a**, and **6** in [D$_6$]DMSO (2×10^{-3} M) at 299 K.

	$D^{[a]}\times10^{-10}$		$D^{[a]}\times10^{-10}$
DMSO	6.55	**2b**	–[b]
1a	6.58	**6**	6.57
2a	6.54		

[a] Experimental error is approximately ±2%. [b] The D value for the solvent in a solution of **2b** in [D$_6$]DMSO could not be determined, because the signal from the residual protonated solvent was superimposed with signals from **2b**.

Molecular models: To compare the expected sizes of our molecules with the results from the diffusion measurements, we have used the program MacroModel® 8.1 (AMBER* force field) to build molecular models of the new compounds.

For **2a·2a**, the results from the molecular modeling conducted in $CHCl_3$ led to the energy-minimized structure depicted in Figure 6 (the energy-minimized structure for **2b·2b** can be found in the Supporting Information). The calculated structure for **2a·2a** reveals a pair of classical capsular aggregates of "almost S_6 symmetry", linked by two hexamethylene tethers. However, this is only one of, eventually, many local energy minima. This variety of conformations, together with the possibility of different diastereomers arising from the clockwise or counterclockwise orientation of each ring of the hydrogen-bonded ureas in **2·2**[22] might explain the multiple resonances found in the ^{1}H NMR spectrum of these species in $CDCl_3$.

It has not been possible to obtain a convergent energy-minimized structure for the self-assembled monomers from **2a** and **2b**, which have not been detected in the ^{1}H NMR spectra taken in $CDCl_3$. It seems that such a folded conformation for these hexaureas, to afford unimolecular capsules, is strongly disfavored.

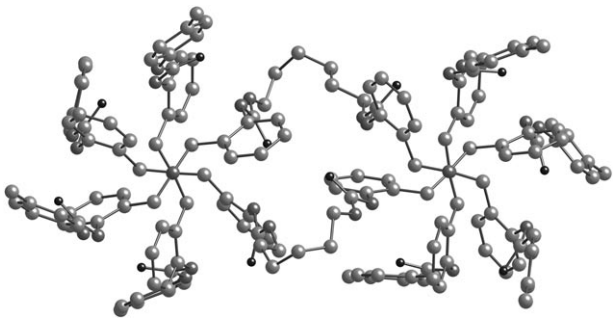

Figure 6. Energy-minimized structure (MacroModel® 8.1, AMBER* force field) of **2a·2a**. All hydrogen atoms have been omitted for clarity.

The files generated in MacroModel® were introduced into the Chem 3D® program, in which the molecular radii can be estimated by measuring distances between atoms. In addition to **2a·2a** and **2b·2b**, an energy-minimized model of **1a·1a** was also generated in Chem 3D®. For these elongated molecules, the hydrodynamic radii in $CDCl_3$ were considered to be approximately 85% of the rotational radii, according to a suggestion made by Mattison et al.[23] In spite of the crude approach,[23] the estimated hydrodynamic radii (Table 4) are in fairly good agreement with the results from the PGSE measurements.

Table 4. Estimated hydrodynamic radii for the dimeric assemblies.

	r_H (model)[a] [Å]	r_H (PGSE)[b] [Å]
1a·1a	7.6	7.8
2a·2a	12.3	12.4
2b·2b	13.5	13.0

[a] Determined by Chem 3D® from the calculated structures in $CDCl_3$. [b] Determined from the *D* values in $CDCl_3$.

Exchange processes and NOE: The ROESY spectrum of a solution of **2a** in $CDCl_3$ (Figure 7a) shows NOE cross-peaks between the methyl and the *ortho*-protons of the *p*-tolyl groups (marked by arrows in the figure). These contacts confirm that these *ortho*-protons resonate at approximately $\delta =$ 7.00 ppm for the nonassembled monomer **2a** (**M** in figure 7a), and at a lower frequency, approximately $\delta = 6.50$ ppm, for the dimer **2a·2a** (**D** in the figure). The other encircled peaks in the figure mark the NOE cross-peaks between the *ortho*- and *meta*-protons of the *p*-tolyl groups in **2a·2a**, as well as between the *meta*-protons and the adjacent NH groups, at approximately $\delta =$ 8.00 ppm. This high NH chemical shift is typical for ureido NH groups engaged in strong hydrogen bonding (in **1a·1a**, these NH protons appear at $\delta = 7.94$ ppm).

The cross-peaks surrounded by rectangles in Figure 7a are particularly important, as they support the capsular geometry proposed for **2a·2a** in $CDCl_3$. These cross-peaks correlate the protons associated with the tribenzylamine moiety (methylene groups at $\delta = 3.10$–3.60 ppm and aromatic protons at $\delta = 7.00$–7.50 ppm) with the aromatic protons of the pendant *p*-tolyl groups of **2a·2a** (at approximately $\delta = 6.20$ and 6.50 ppm). By analogy to **1a** (see Figure S1 in the Supporting Information),[10c] these interactions point to a dimeric, bicapsular structure, **2a·2a**, in which the *p*-tolyl groups of one **2a** molecule are close to the tribenzylamine moiety of the other.

Figure 7b shows the ROESY spectrum for a solution of **2b** in $CDCl_3$. The black arrow in the figure marks, for **2b·2b**, the intramolecular NOEs between the *ortho* and the methylene protons of the *p*-BuC_6H_4 groups. The weak cross-peak marked by the white arrow might correspond to the analogous interaction within the monomer **2b**, which is present at a very low concentration in this solution. The rectangles in Figure 7b surround the peaks assigned to intermolec-

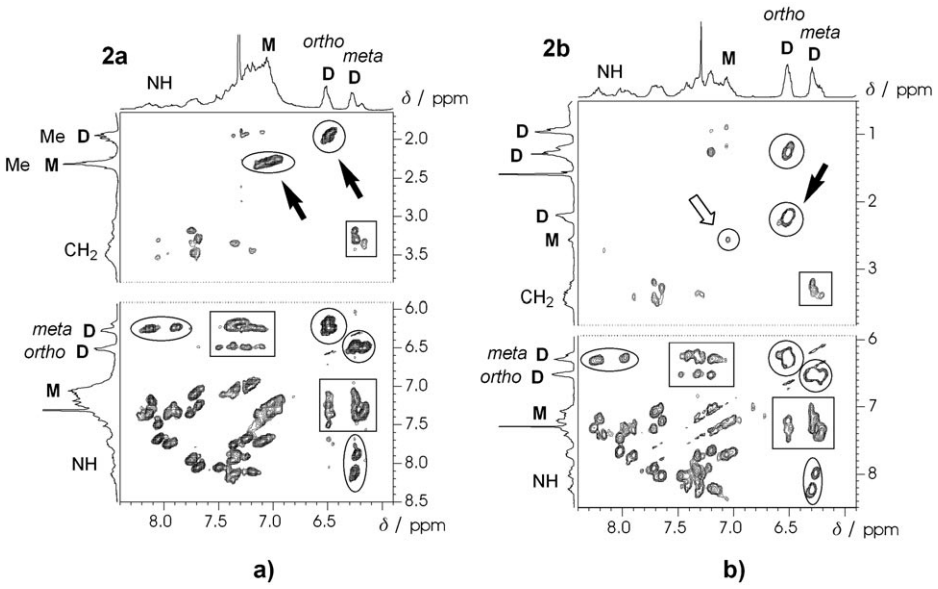

Figure 7. a) ROESY spectrum of a solution of **2a** in $CDCl_3$ (500 MHz, 2×10^{-3} M), showing the cross-peaks resulting from the NOE contacts within the monomer **2a** (**M**) and the dimer **2a·2a** (**D**). The cross-peaks between the *ortho*-protons and the methyl protons of the *p*-tolyl groups are marked with arrows. The intramolecular cross-peaks within each unit of **2a** in **2a·2a** are surrounded with circles and ellipses, while the intermolecular cross-peaks between the two units of **2a** in **2a·2a** are marked with rectangles. b) ROESY spectrum of a $CDCl_3$ solution of **2b** (500 MHz, 5×10^{-3} M), showing the cross-peaks resulting from the NOE contacts within the monomer **2b** (**M**) and the dimer **2b·2b** (**D**). The contacts between the *ortho* and some of the methylene protons of the BuC_6H_4 groups are marked with arrows. The intramolecular cross-peaks within each unit of **2b** in **2b·2b** are surrounded with circles and ellipses, while the intermolecular cross-peaks between the two units of **2b** in **2b·2b** are marked with rectangles.

ular NOE interactions between the tribenzylamine moiety and the *p*-BuC_6H_4 groups, which provides further evidence for the capsular structure of **2b·2b**.

All the protons involved in intermolecular NOE contacts within **2a·2a** and **2b·2b** are separated by less than 3.50 Å in the energy-minimized structures. When no intermolecular NOE cross-peaks are observed (e.g., between the methylenic protons of the tribenzylamine moiety and the protons *ortho* to the Me/Bu substituents), the interatomic distances in the models are larger than 3.50 Å.

ESI mass spectra: The ESI mass spectrum of the hexaurea **2a** measured in $CHCl_3$ (1.00 mM) produced a base peak corresponding to $[\mathbf{2a{\cdot}2a}+H]^+$ at $m/z=2730$ and the signal for the protonated monomer at $m/z=1366$ (Figure 8a).[24] The

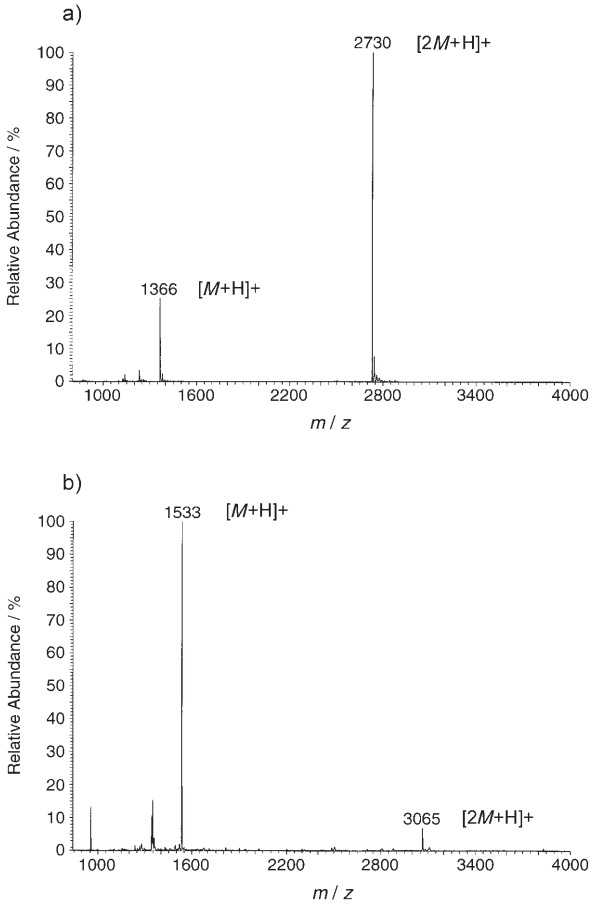

Figure 8. ESI mass spectrum, in the range of 800–4000, of a $CHCl_3$ solution (1.00 mM) of a) **2a** and b) **2b**.

MS/MS (magnetic sector mass spectrometry) spectrum for the signal at $m/z=2730$ was also measured and produced a peak at $m/z=1365$, which was assigned to the monomer.

For **2b**, the ESI mass spectrum in $CHCl_3$ (1.00 mM) produced a signal for the protonated dimer $[\mathbf{2b{\cdot}2b}+H]^+$ at $m/z=3065$ (Figure 8b).[24] In addition, the signal for the protonated monomer was also observed as the base peak at $m/z=1533$. In this case a MS/MS spectrum of the signal at $m/z=3065$ could not be measured due to its low intensity.

Equilibria: 1D NMR spectroscopic saturation experiments on a solution of **2a** in $CDCl_3$ did not reveal saturation transfer between the methyl signals of the monomer and dimer, pointing to a rate constant for the exchange that is smaller than 0.01 s^{-1}. Similarly, the ROESY spectra of **2a** and **2b** in $CDCl_3$ (Figure 7) did not show cross-peaks due to exchange processes.

Nevertheless, we have observed that an increase in concentration favors the formation of the dimer (compare the two spectra of **2a** in Figure 3). The equilibrium is reached within minutes, and the ratio of species remains unchanged for more than one month. For **2b**, the equilibrium is displaced towards the dimer.

To provide semiquantitative data on the relative stability of the dimers, their solutions in $CDCl_3$ were titrated with $[D_6]$DMSO, and the process followed by ^{1}H NMR spectroscopic analysis. For **2a·2a**, 2% vol $[D_6]$DMSO was required for 50% dissociation (i.e. [Dimer]/[Monomer]≅1), while for **1a·1a** and **1b·1b** 8–9% vol $[D_6]$DMSO was required to reach the same level of dissociation. These results reflect the lower stability of **2a·2a** relative to **1a·1a** and **1b·1b**. For **2b·2b**, the point of 50% dissociation cannot be distinguished by ^{1}H NMR spectroscopy, as a result of the superposition of the signals from the monomer and dimer. However, titration with $[D_6]$DMSO until the point of complete dissociation afforded a result of 19% vol $[D_6]$DMSO[25] needed for **2a·2a**, versus 29% vol $[D_6]$DMSO for **2b·2b,**[25] indicating the higher relative stability of the later. For **1a·1a** and **1b·1b** 33–34% vol $[D_6]$DMSO was required for total destruction of the dimer.[10a,c,25] The dimers of calix[4]arenes, bearing four urea functions at the wider rim, are usually destroyed by 2–10% vol of DMSO added to an apolar solvent.[19b,26]

The dimerization constant (K_D)[27] for **2a**, was determined at three different concentrations (0.040–0.020 M) from the integrals of the ^{1}H NMR spectrum measured at 298 K, and gave values of 440, 540, and 610 M^{-1}. However, these numbers can be taken only as a rough estimate, since the K_D values increased with the decreasing concentration of the hexaurea. These results points to the presence of small quantities of oligomeric species, which may lead to very broad and undetectable signals in the ^{1}H NMR spectra (see above).[26c]

We had previously observed[10c] that the stability of the dimers **1·1** is strongly dependent on the terminal substituents of the urea functionality ($K_D=91200\ M^{-1}$ for **1a** and $K_D=4000\ M^{-1}$ for **1c**) and, to lesser extent, on the substituents located on the tribenzylamine skeleton ($K_D=1000\ M^{-1}$ for **1d**). The K_D value found for the hexaurea **2a** is slightly lower than that of the triurea **1d**.

Conclusion

The hexaureas **2a**,**b**, formed by two tris(2-ureidobenzyl)amine moieties linked by an hexamethylene tether, are prone to assemble in $CDCl_3$ to afford bicapsular dimeric aggregates, **2a·2a** and **2b·2b**, which both contain two rings of six hydrogen-bonded ureas. In solution, these dimers are in equilibrium with the nonassembled monomers **2a** and **2b**, but show kinetic stability on the NMR timescale. No polymers or self-assembled monomers were detected in $CDCl_3$, at least not in measurable concentrations. The thermodynamic stabilities of **2a·2a** and **2b·2b** are comparable to those of other capsular aggregates derived from tribenzylamines. The characterization of these new supramolecules in solution was carried out by ^{1}H NMR and ^{1}H/^{1}H-ROESY spectroscopic studies, and PGSE diffusion studies. The PGSE diffusion methodology has been shown once more to be an extremely efficient tool for studying supramolecular interactions in solution. As far as we know, the dimeric species **2·2** constitutes as a unique example of a bicapsular aggregate, which is associated strictly by hydrogen bonding. This new type of assembly demonstrates the efficiency of the tribenzylamine subunit in the design of new supramolecular systems.

Experimental Section

General: ^{1}H and ^{13}C NMR spectra were measured on Bruker AC 200 (^{1}H: 200 MHz, ^{13}C: 50 MHz), Varian Unity-300 (^{1}H: 300 MHz, ^{13}C: 75 MHz), Bruker AVANCE 600 (^{1}H: 600 MHz, ^{13}C: 151 MHz), and Bruker AVANCE 700 (^{1}H: 700 MHz) spectrometers with TMS ($\delta=0.00$ ppm) or the solvent residual peak as internal standards. IR spectra were recorded on a FT–IR Nicolet Impact 400 infrared spectrometer and melting points were taken on a Reichert apparatus and are not corrected.

The PGSE NMR diffusion measurements were carried out by using the stimulated echo pulse sequence,[18b] as has been explained elsewhere.[17c,28] All the experiments were performed on a 500 MHz Bruker AVANCE spectrometer, equipped with a microprocessor-controlled gradient unit and a multinuclear inverse probe with an actively shielded Z-gradient coil. The sample was not spun and the airflow was disconnected. The shape of the gradient pulse was rectangular, and its strength varied automatically during the course of the experiments. The D values were determined from the slope of the regression line $\ln(I/I_o)$ versus G^2, according to Equation (1).

$$\ln(I/I_o) = -(\gamma\delta)^2 G^2(\Delta\text{-}\delta/3)D \quad (1)$$

In Equation (1) I/I_o = observed spin echo intensity/intensity without gradients, G = gradient strength, Δ = delay between the midpoints of the gradients, D = diffusion coefficient, and δ = gradient length.

The calibration of the gradients was carried out by a diffusion measurement of HDO in D_2O ($D_{HDO}=1.9\times10^{-9}$ m^2 s^{-1}).[29] The values reported in Tables 1–3 are an average of three different measurements, which yielded D values within a maximum of ±1.5% of the reported value. All the measurements were carried out by using the ^{1}H NMR spectroscopic resonances. For the measurements in $CDCl_3$, the gradient length (δ) was set to 1.75 ms and the diffusion delay was set to approximately 68, 93, and 168 ms. For the experiments in [D$_6$]DMSO the diffusion delays were longer (approximately 168, 218, and 268 ms), to compensate for the higher viscosity of this solvent. The relaxation delay was always 5 s and the number of scans 16 (except for the measurements on the signal at $\delta=2.5$ ppm, in the $CDCl_3$ solution of **2b**, for which 80 scans per increment were required). Typically, 14–20 points were used for the regression analysis and the experimental time was approximately 40 min. All of the observed data leading to the reported D values afforded lines whose correlation coefficients were above 0.999.

All molecular mechanics calculations were carried out by using the AMBER* force field as implemented within Maestro/MacroModel® 8.1. Standard potentials and atomic charges, as provided by the AMBER* force field, were employed without modifications. AMBER* and OPLAA force fields produce essentially the same results in related structures. Calculations were initially performed under vacuum and then in chloroform (GB/SA solvation model). Most complex structures were virtually identical under both conditions. Energy minimizations were conducted over 500 iterations on a silicon graphics computer. Minimized structures were then subjected to conformational searches with 5000-step Monte Carlo multiple minimum simulations. All conformations within 15 kJ mol^{-1} of the computed global minimum were stored, and the representative lowest energy structure was analyzed.

The ROESY experiments were measured on solutions of **2a** (2×10^{-3} M) and **2b** (5×10^{-3} M) in $CDCl_3$, with a 500 MHz Bruker AVANCE spectrometer, equipped with a multinuclear inverse probe. A spin-lock pulse of 400 ms was used. The number of scans was 128 for **2a** and 280 for **2b**. Total experimental times were approximately 20 h.

CAUTION: Azido compounds may represent an explosion hazard when being concentrated under vacuum or stored neat. A safety shield and appropriate handling procedures are recommended.

Bis(2-nitrobenzyl)(2-azidobenzyl)amine (3): 2-Azidobenzylamine[30] (1.60 g, 10.8 mmol) and 2-nitrobenzyl iodide[10c] (5.68 g, 21.6 mmol) were added, as solutions in dry acetonitrile (2 and 5 mL respectively), to a suspension of Na_2CO_3 (6.58 g, 62.1 mmol) in acetonitrile (10 mL), and the reaction mixture stirred under reflux for 24 h. After cooling, the inorganic salts were filtered and washed with cold acetonitrile (5×5 mL). The filtrate was collected, the solvent was removed, and the residue was purified by silica-gel chromatography, eluting with EtOAc/hexanes 1:6 ($R_f=0.34$), to afford **3** (93 % yield) as pale yellow prisms (an analytical sample was obtained by recrystallization from CH_2Cl_2/Et_2O 1:3). M.p. 84–85 °C; ^{1}H NMR (200 MHz, $CDCl_3$, 25 °C, TMS): $\delta=3.55$ (s, 2H), 3.91 (s, 4H), 7.04–7.11 (m, 2H), 7.22–7.37 (m, 4H), 7.51 (td, ^3J(H,H) = 7.5 Hz, ^4J(H,H) = 1.3 Hz, 2H), 7.65 (dd, ^3J(H,H) = 7.7 Hz, ^4J(H,H) = 1.1 Hz, 2H), 7.78 ppm (dd, ^3J(H,H) = 8.0 Hz, ^4J(H,H) = 1.3 Hz, 2H); ^{13}C NMR (50 MHz, $CDCl_3$, 25 °C): $\delta=54.2$ (t), 55.6 (2t), 118.1 (d), 124.3 (2d), 124.6 (d), 127.9 (2d), 128.6 (s), 128.9 (d), 131.0 (2d), 131.4 (d), 132.6 (2d), 134.1 (2s), 138.9 (s), 149.6 ppm (2s); IR (Nujol): $\tilde{\nu}=2131$ (N_3), 1531 (NO_2), 1522, 1342 cm^{-1} (NO_2); MS (70 eV, EI): *m/z* (%): 419 (43) $[M+1]^+$, 418 (11) $[M]^+$, 286 (66), 105 (100); elemental analysis calcd (%) for $C_{21}H_{18}N_6O_4$ (418.4): C 60.28, H 4.34, N 20.09; found: C 60.01, H 4.50, N 20.45.

Bis(2-nitrobenzyl)(2-aminobenzyl)amine (4): PMe_3 in toluene (1.0 M, 11.7 mL, 11.7 mmol) was slowly added at 0 °C to a solution of **3** (4.10 g, 9.8 mmol) in freshly distilled THF (30 mL) under N_2. The reaction mixture was then stirred at this temperature for 30 min. After this time, H_2O (15 mL) was added and the reaction mixture was stirred at 20 °C for a further 20 h. After removal of the organic solvent, H_2O (40 mL) was added and the aqueous phase was extracted with CH_2Cl_2 (3×20 mL). The combined extracts were dried over $MgSO_4$, the solvent was evaporated, and the residue was purified by silica-gel chromatography, eluting with EtOAc/hexanes 1:4 ($R_f=0.16$), to afford **4** (67–90 % yield) as yellow prisms (an analytical sample was obtained by recrystallization from $CHCl_3$/Et_2O 1:4). M.p. 96–99 °C; ^{1}H NMR (200 MHz, $CDCl_3$, 25 °C, TMS): $\delta=3.55$ (s, 2H), 3.85 (s, 4H), 4.13 (s, 2H), 6.53–6.65 (m, 2H), 6.98–7.06 (m, 2H), 7.22–7.31 (m, 2H), 7.37–7.48 (m, 4H), 7.66 ppm (dd, ^3J(H,H) = 8.1 Hz, ^4J(H,H) = 1.0 Hz, 2H); ^{13}C NMR (50 MHz, $CDCl_3$, 25 °C): $\delta=56.3$ (2t), 59.4 (t), 115.6 (d), 117.8 (d), 121.4 (s), 124.2 (2d), 128.2 (2d), 128.9 (d), 131.2 (d), 132.0 (2d), 132.6 (2d), 133.4 (2s), 146.5 (s), 149.7 ppm (2s); IR (Nujol): $\tilde{\nu}=3486$ (NH), 3390 (NH), 1623, 1522 (NO_2), 1340 cm^{-1} (NO_2); MS (70 eV, EI): *m/z* (%): 393 (42) $[M+1]^+$, 375

(39), 286 (47), 257 (82), 120 (100); HRMS (EI): *m/z*: calcd for $C_{21}H_{20}N_4O_4$: 392.148455; found 392.148647; elemental analysis calcd (%) for $C_{21}H_{20}N_4O_4$ (392.4): C 64.28, H 5.14, N 14.28; found: C 64.05, H 5.15, N 14.33.

1-{2-{[Bis(2-nitrobenzyl)amino]methyl}phenyl}-3-{6-{3-{2-{[bis(2-nitrobenzyl)amino]methyl}phenyl}ureido}hexyl}urea (5): 1,6-Diisocyanatohexane (0.42 g, 2.5 mmol) was added, under N_2, to a solution of the amine **4** (1.94 g, 4.9 mmol) in dry $CHCl_3$ (60 mL). After stirring at 100 °C for 30 h in a sealed tube the solvent was removed and the residue was purified by silica-gel chromatography, eluting with EtOAc/hexanes 1:1→4:1 (R_f= 0.16 in EtOAc/hexanes 1:1), to afford **5** (69 % yield) as pale yellow prisms (an analytical sample was obtained by recrystallization from CH_2Cl_2/Et_2O 1:1). M.p. 99–104 °C; ^{1}H NMR (300 MHz, $CDCl_3$, 25 °C, TMS): δ = 1.52–1.54 (m, 4H), 1.65–1.71 (m, 4H), 3.37 (q, ^3J(H,H) = 6.5 Hz, 4H), 3.69 (s, 4H), 3.90 (s, 8H), 5.77 (t, ^3J(H,H) = 5.3 Hz, 2H), 6.85 (td, ^3J(H,H) = 7.5 Hz, ^4J(H,H) = 1.1 Hz, 2H), 7.07 (dd, ^3J(H,H) = 7.4 Hz, ^4J(H,H) = 1.4 Hz, 2H), 7.13–7.25 (m, 10H), 7.38 (td, ^3J(H,H) = 7.6 Hz, ^4J(H,H) = 1.2 Hz, 4H), 7.44 (s, 2H), 7.59 (dd, ^3J(H,H) = 8.1 Hz, ^4J(H,H) = 1.2 Hz, 4H), 7.96 ppm (dd, ^3J(H,H) = 8.1 Hz, ^4J(H,H) = 0.6 Hz, 2H); ^{13}C NMR (75 MHz, $CDCl_3$, 25 °C): δ = 26.7 (2t), 30.0 (2t), 40.2 (2t), 57.3 (4t), 61.2 (2t), 121.1 (2d), 121.9 (2d), 124.3 (4d), 124.6 (2s), 128.2 (4d), 129.0 (2d), 130.9 (2d), 132.0 (4d), 133.1 (4d), 133.4 (4s), 139.2 (2s), 148.9 (4s), 155.4 ppm (2s); IR (Nujol): $\tilde{\nu}$ = 3297 (NH), 1622 (C=O), 1522 (NO_2), 1342 cm^{-1} (NO_2); MS (FAB): *m/z* (%): 953 (12) $[M+1]^+$, 818 (10), 666 (12), 419 (49), 106 (100); elemental analysis calcd (%) for $C_{50}H_{52}N_{10}O_{10}$ (953.0): C 63.01, H 5.50, N 14.70; found: C 63.05, H 5.56, N 14.71.

1-{2-{[Bis(2-aminobenzyl)amino]methyl}phenyl}-3-{6-{3-{2-{[bis(2-aminobenzyl)amino]methyl}phenyl}ureido}hexyl}urea (6): PtO_2 (0.67 g, 2.9 mmol) was added to a solution of **5** (1.40 g, 1.5 mmol) in freshly distilled THF (100 mL), and the resulting reaction mixture was stirred at 20 °C for 20 h under H_2. After filtration over a pad of celite, the solvent was removed to afford the tetraamine **6** (91 % yield) as colorless prisms. This compound was deemed pure enough for the following step (an analytical sample was obtained by recrystallization from CH_2Cl_2/Et_2O 1:2). Compound **6** could not be completely dried, even by placing under a high temperature (100 °C) and vacuum (0.15 Torr). M.p. 126–128 °C; ^{1}H NMR (300 MHz, $CDCl_3$, 25 °C, TMS): δ = 1.36–1.44 (m, 4H), 1.52–1.56 (m, 4H), 3.19 (q, ^3J(H,H) = 6.5 Hz, 4H), 3.41 (s, 8H), 3.48 (s, 4H), 3.83 (br s, 8H), 6.01 (t, ^3J(H,H) = 5.6 Hz, 2H), 6.61 (dd, ^3J(H,H) = 8.4 Hz, ^4J(H,H) = 0.9 Hz, 4H), 6.73 (td, ^3J(H,H) = 7.4 Hz, ^4J(H,H) = 1.0 Hz, 4H), 6.88 (td, ^3J(H,H) = 7.5 Hz, ^4J(H,H) = 1.0 Hz, 2H), 7.06–7.12 (m, 10H), 7.18 (td, ^3J(H,H) = 7.8 Hz, ^4J(H,H) = 1.5 Hz, 2H), 7.81 (s, 2H), 8.03 ppm (d, ^3J(H,H) = 8.1 Hz, 2H); ^{13}C NMR (75 MHz, $CDCl_3$, 25 °C): δ = 26.3 (2t), 30.0 (2t), 39.6 (2t), 56.9 (4t), 58.0 (2t), 116.3 (4d), 118.8 (4d), 120.9 (2d), 121.80 (2d), 121.84 (4s), 124.9 (2s), 128.8 (2d), 129.3 (4d), 131.0 (2d), 132.4 (4d), 138.7 (2s), 144.8 (4s), 155.5 ppm (2s); IR (Nujol): $\tilde{\nu}$ = 3373 (NH), 3313 (NH), 1677 cm^{-1} (C=O); MS (FAB): *m/z* (%): 833 (7) $[M+1]^+$, 359 (7), 106 (100); elemental analysis calcd (%) for $C_{50}H_{60}N_{10}O_2 \cdot H_2O$ (851.1): C 70.56, H 7.34, N 16.46; found: C 70.48, H 7.13, N 16.53.

Hexaurea 2a: 4-Methylphenyl isocyanate (0.22 g, 1.68 mmol) was added, under N_2, to a solution of **6** (0.35 g, 0.42 mmol) in dry $CHCl_3$ (20 mL). After stirring under reflux for 24 h the solvent was removed and the residue was purified by silica-gel chromatography, eluting with EtOAc/hexanes 1:3 (to remove *N*,*N*′-bis(4-methylphenyl)urea) →EtOAc, to afford **2a** (R_f=0.85 in EtOAc; 60 % yield) as colorless prisms (an analytical sample was obtained by recrystallization from CH_2Cl_2/*n*-hexane 1:1). M.p. 176–178 °C; ^{1}H NMR (600 MHz, [D$_6$]DMSO, 25 °C, TMS): δ = 1.20–1.26 (m, 4H), 1.34–1.40 (m, 4H), 2.21 (s, 12H), 3.00 (q, ^3J(H,H) = 6.0 Hz, 4H), 3.56 (s, 4H), 3.59 (s, 8H), 6.29 (br s, 2H), 6.96 (t, ^3J(H,H) = 7.4 Hz, 2H), 7.02–7.05 (m, 12H), 7.09 (t, ^3J(H,H) = 7.6 Hz, 2H), 7.17 (t, ^3J(H,H) = 7.6 Hz, 4H), 7.29 (d, ^3J(H,H) = 8.3 Hz, 8H), 7.46 (d, ^3J(H,H) = 7.4 Hz, 2H), 7.51 (d, ^3J(H,H) = 7.5 Hz, 4H), 7.53 (d, ^3J(H,H) = 8.2 Hz, 2H), 7.56 (d, ^3J(H,H) = 8.0 Hz, 4H), 7.71 (s, 2H), 7.86 (s, 4H), 8.67 ppm (s, 4H); ^{13}C NMR (151 MHz, [D$_6$]DMSO, 25 °C): δ = 20.3 (q), 26.2 (t), 29.7 (t), 39.3 (t), 54.4 (t), 54.7 (t), 118.2 (d), 123.0 (d), 123.5 (d), 123.6 (d), 127.1 (d), 128.8 (d), 129.0 (s), 129.1 (d), 129.6 (s), 130.5 (s), 137.1 (s), 137.2 (s), 137.9 (s), 152.9 (s), 155.9 ppm (s), three signals are overlapped; IR (Nujol): $\tilde{\nu}$ = 3324 (NH), 1655 cm^{-1} (C=O); MS (FAB): *m/z* (%): 1364 (4) $[M]^+$, 625 (11), 239 (89), 132 (100); elemental analysis calcd (%) for $C_{82}H_{88}N_{14}O_6$ (1365.7): C 72.12, H 6.49, N 14.36; found: C 71.62, H 6.52, N 14.50.

Hexaurea 2b: 4-Butylphenyl isocyanate (0.21 g, 1.20 mmol) was added, under N_2, to a solution of **6** (0.25 g, 0.30 mmol) in dry $CHCl_3$ (25 mL). After stirring under reflux for 24 h the solvent was removed and the residue purified by recrystallization from EtOH to afford **2b** (58 % yield) as colorless prisms. M.p. 164–166 °C; ^{1}H NMR (600 MHz, [D$_6$]DMSO, 25 °C, TMS): δ = 0.86 (t, ^3J(H,H) = 7.4 Hz, 12H), 1.22–1.29 (m, 12H), 1.37 (m, 4H), 1.49 (quint, ^3J(H,H) = 7.6 Hz, 8H), 2.47 (t, ^3J(H,H) = 7.6 Hz, 8H), 2.99 (q, ^3J(H,H) = 6.0 Hz, 4H), 3.56 (s, 4H), 3.58 (s, 8H), 6.28 (br s, 2H), 6.95 (t, ^3J(H,H) = 7.4 Hz, 2H), 7.03–7.04 (m, 12H), 7.08 (t, ^3J(H,H) = 7.6 Hz, 2H), 7.17 (t, ^3J(H,H) = 7.5 Hz, 4H), 7.29 (d, ^3J(H,H) = 8.4 Hz, 8H), 7.46 (d, ^3J(H,H) = 7.4 Hz, 2H), 7.50 (d, ^3J(H,H) = 7.5 Hz, 4H), 7.53 (d, ^3J(H,H) = 8.1 Hz, 2H), 7.56 (d, ^3J(H,H) = 8.0 Hz, 4H), 7.70 (s, 2H), 7.86 (s, 4H), 8.66 ppm (s, 4H); ^{13}C NMR (151 MHz, [D$_6$]DMSO, 25 °C): δ = 13.8 (q), 21.7 (t), 26.2 (t), 29.7 (t), 33.3 (t), 34.2 (t), 39.3 (t), 54.5 (t), 54.7 (t), 118.2 (d), 123.0 (d), 123.6 (d), 127.2 (d), 128.4 (d), 128.8 (d), 129.0 (d), 129.1 (s), 129.6 (s), 135.6 (s), 137.1 (s), 137.3 (s), 137.9 (s), 153.0 (s), 155.8 ppm (s), three signals are overlapped; IR (Nujol): $\tilde{\nu}$ = 3310 (NH), 1653 cm^{-1} (C=O); MS (FAB): *m/z* (%): 1534 (1) $[M+1]^+$, 709 (6), 281 (100); elemental analysis calcd (%) for $C_{94}H_{112}N_{14}O_6$ (1534.0): C 73.60, H 7.36, N 12.78; found: C 73.24, H 7.42, N 12.81.

Acknowledgements

This work was supported by MCYT-FEDER (Project BQU2001–0010), Fundación Séneca-CARM (Project 00458/PI/04), the Swiss National Science Foundation, and the ETH Zurich. A.P. is grateful to the Ministerio de Educación y Ciencia of Spain and the University of Murcia (Spain) for a *Ramón y Cajal* contract. R.-A.O. thanks the Fundación Cajamurcia for a fellowship. E.M.-V. thanks the Fundación Séneca-CARM for a grant. We thank Dr. Heinz Rüegger for the helpful discussions and advice about the NMR measurements, as well as for the acquisition of the 700 MHz ^{1}H NMR spectrum of **2a**.

[1] a) C. A. Schalley, *Adv. Mater.* **1999**, *11*, 1535–1537; b) R. P. Sijbesma, E. W. Meijer, *Curr. Opin. Colloid Interface Sci.* **1999**, *4*, 24–32; c) L. J. Prins, D. N. Reinhoudt, P. Timmerman, *Angew. Chem.* **2001**, *113*, 2446–2492; *Angew. Chem. Int. Ed.* **2001**, *40*, 2382–2426; d) E. A. Archer, A. E. Sochia, M. J. Krische, *Chem. Eur. J.* **2001**, *7*, 2059–2065.

[2] S. J. Geib, C. Vicent, E. Fan, A. D. Hamilton, *Angew. Chem.* **1993**, *105*, 83–85; *Angew. Chem. Int. Ed. Engl.* **1993**, *32*, 119–121.

[3] G. M. Whitesides, E. E. Simanek, J. P. Mathias, C. T. Seto, D. N. Chin, M. Mammen, D. M. Gordon, *Acc. Chem. Res.* **1995**, *28*, 37–44.

[4] M. R. Ghadiri, J. R. Granja, R. A. Milligan, D. E. McRee, N. Khazanovich, *Nature* **1993**, *366*, 324–327.

[5] a) M. M. Conn, J. Rebek, Jr., *Chem. Rev.* **1997**, *97*, 1647–1668; b) V. Böhmer, M. O. Vysotsky, *Aust. J. Chem.* **2001**, *54*, 671–677; c) F. Hof, S. L. Craig, C. Nuckolls, J. Rebek, Jr., *Angew. Chem.* **2002**, *114*, 1556–1578; *Angew. Chem. Int. Ed.* **2002**, *41*, 1488–1508.

[6] S. C. Zimmerman, F. Zeng, D. E. C. Reichert, S. V. Kolotuchin, *Science* **1996**, *271*, 1095–1098.

[7] a) R. P. Sijbesma, F. H. Beijer, L. Brunsveld, B. J. B. Folmer, J. H. K. Ky Hirschberg, R. F. M. Lange, J. K. L. Lowe, E. W. Meijer, *Science* **1997**, *278*, 1601–1604; b) H.-A. Klok, K. A. Jolliffe, C. L. Schauer, L. J. Prins, J. P. Spatz, M. Möller, P. Timmerman, D. N. Reinhoudt, *J. Am. Chem. Soc.* **1999**, *121*, 7154–7155; c) R. K. Castellano, J. Rebek, Jr., *J. Am. Chem. Soc.* **1998**, *120*, 3657–3663; d) R. K. Castellano, C. Nuckolls, S. H. Eichhorn, M. R. Wood, A. J. Lovinger, J. Rebek, Jr., *Angew. Chem.* **1999**, *111*, 2764–2768; *Angew. Chem. Int. Ed.* **1999**, *38*, 2603–2606; e) R. K. Castellano, R. Clark, S. L. Craig,

C. Nuckolls, J. Rebek, Jr., *Proc. Natl. Acad. Sci. USA* **2000**, *97*, 12418–12421.
[8] P. Lipkowski, A. Bielejewska, H. Kooijman, A. L. Spek, P. Timmerman, D. N. Reinhoudt, *Chem. Commun.* **1999**, 1311–1312.
[9] a) M. C. Etter, Z. Urbañczyk-Lipkowska, M. Zia-Ebrahimi, T. W. Panunto, *J. Am. Chem. Soc.* **1990**, *112*, 8415–8426; b) X. Zhao, Y.-L. Chang, F. W. Fowler, J. W. Lauher, *J. Am. Chem. Soc.* **1990**, *112*, 6627–6634; c) J. J. Kane, R.-F. Liao, J. W. Lauher, F. W. Fowler, *J. Am. Chem. Soc.* **1995**, *117*, 12003–12004; d) S. Boileau, L. Bouteiller, F. Lauprête, F. Lortie, *New J. Chem.* **2000**, *24*, 845–848; e) F. Lortie, S. Boileau, L. Bouteiller, *Chem. Eur. J.* **2003**, *9*, 3008–3014.
[10] a) M. Alajarín, A. López-Lázaro, A. Pastor, P. D. Prince, J. W. Steed, R. Arakawa, *Chem. Commun.* **2001**, 169–170; b) M. Alajarín, A. Pastor, R.-A. Orenes, J. W. Steed, *J. Org. Chem.* **2002**, *67*, 7091–7095; c) M. Alajarín, A. Pastor, R.-A. Orenes, J. W. Steed, R. Arakawa, *Chem. Eur. J.* **2004**, *10*, 1383–1397.
[11] M. S. Brody, C. A. Schalley, D. M. Rudkevich, J. Rebek, Jr., *Angew. Chem.* **1999**, *111*, 1738–1742; *Angew. Chem. Int. Ed.* **1999**, *38*, 1640–1644.
[12] J. M. Rivera, J. Rebek, Jr., *J. Am. Chem. Soc.* **2000**, *122*, 7811–7812.
[13] J. Yoon, D. J. Cram, *Chem. Commun.* **1997**, 2065–2066.
[14] a) N. Chopra, J. C. Sherman, *Angew. Chem.* **1997**, *109*, 1828–1830; *Angew. Chem. Int. Ed. Engl.* **1997**, *36*, 1727–1729; b) N. Chopra, C. Naumann, J. C. Sherman, *Angew. Chem.* **2000**, *112*, 200–202; *Angew. Chem. Int. Ed.* **2000**, *39*, 194–196.
[15] F. Venema, A. E. Rowan, R. J. M. Nolte, *J. Am. Chem. Soc.* **1996**, *118*, 257–258.
[16] Y. Liu, Y. Song, Y. Chen, X.-Q. Li, F. Ding, R.-Q. Zhong, *Chem. Eur. J.* **2004**, *10*, 3685–3696.
[17] a) M. Shaul, Y. Cohen, *J. Org. Chem.* **1999**, *64*, 9358–9364; b) P. Timmerman, J.-L. Weidmann, K. A. Jolliffe, L. J. Prins, D. N. Reinhoudt, S. Shinkai, L. Frish, Y. Cohen, *J. Chem. Soc. Perkin Trans. 2* **2000**, 2077–2089; c) D. G. Regan, B. E. Chapman, P. W. Kuchel, *Magn. Reson. Chem.* **2002**, *40*, S115-S121; d) X. Ribas, J. C. Dias, J. Morgado, K. Wurst, M. Almeida, T. Parella, J. Veciana, C. Rovira, *Angew. Chem.* **2004**, *116*, 4141–4144; *Angew. Chem. Int. Ed.* **2004**, *43*, 4049–4052.
[18] a) E. O. Stejskal, J. E. Tanner, *J. Chem. Phys.* **1965**, *42*, 288–292; b) P. Stilbs, *Prog. Nucl. Magn. Reson. Spectrosc.* **1987**, *19*, 1–45; c) W. S. Price, *Annu. Rep. NMR Spectrosc.* **1996**, *32*, 51–142; d) C. S. Johnson, Jr., *Prog. Nucl. Magn. Reson. Spectrosc.* **1999**, *34*, 203–256.
[19] a) L. Frish, S. E. Matthews, V. Böhmer, Y. Cohen, *J. Chem. Soc. Perkin Trans. 2* **1999**, 669–671; b) L. Frish, M. O. Vysotsky, S. E. Matthews, V. Böhmer, Y. Cohen, *J. Chem. Soc. Perkin Trans. 2* **2002**, 88–93; c) L. Avram, Y. Cohen, *Org. Lett.* **2002**, *4*, 4365–4368; d) L. Avram, Y. Cohen, *J. Am. Chem. Soc.* **2002**, *124*, 15148–15149; e) L. Avram, Y. Cohen, *Org. Lett.* **2003**, *5*, 1099–1102; f) L. Frish, M. O. Vysotsky, V. Böhmer, Y. Cohen, *Org. Biomol. Chem.* **2003**, *1*, 2011–2014.
[20] The Stokes–Einstein: $D=(k_BT)/(6\pi\eta r)$. In this equation, D = diffusion coefficient, k_B = Boltzman constant, T = temperature in degrees Kelvin, η = viscosity of the solution (for diluted solutions, the viscosity of the solvent can be used), and r = hydrodynamic radius (the radius of a hypothetical hard sphere that diffuses with the same speed as the particle under examination). See: J. T. Edward, *J. Chem. Educ.* **1970**, *47*, 261–270.
[21] M. Valentini, H. Rüegger, P. S. Pregosin, *Helv. Chim. Acta* **2001**, *84*, 2833–2853.
[22] The reorientation of the hydrogen-bonded urea groups would be slow on the NMR timescale; this is analogous to what is observed for the dimers **1·1** (otherwise, averaged C_{3v} symmetries would be observed).
[23] The rotational radius (r_r) is the radius of the sphere determined by rotating a molecule around its geometric center. The r_r values are usually too big when compared with r_H. See: K. W. Mattison, U. Nobbmann, D. Dolak, *Am. Biotechnol. Lab.* **2001**, *19*, 66–67. We have taken the average of the two longest diagonals of the molecule.
[24] These masses are not isotopic but averaged due to the low resolution of the equipment in the range of 800–4000 Da. For **2a** the calculated values for the averaged masses of the protonated dimer and monomer are 1366 and 2732, respectively. For **2b** the calculated values are 1535 and 3069, respectively. Although the spectrometer was calibrated before the measurements, there is a slight difference (2–4 Da) between the calculated and the experimental values, which may due to technical problems encountered with the equipment in this mass range.
[25] The percentage of [D_6]DMSO is given with respect to the overall volume ([D_6]DMSO + $CDCl_3$), while in references [10a,c] the percentage of [D_6]DMSO relative to the volume of $CDCl_3$ was given. In these experiments, [D_6]DMSO was added to a solution of $CDCl_3$ until the monomer/dimer ratio = 95:5 (300 MHz) in the ^{1}H NMR spectra. In the mixture $CDCl_3$/[D_6]DMSO the monomer/dimer equilibrium remains slow on the NMR timescale.
[26] a) O. Mogck, M. Pons, V. Böhmer, W. Vogt, *J. Am. Chem. Soc.* **1997**, *119*, 5706–5712; b) M. O. Vysotsky, I. Thondorf, V. Böhmer, *Chem. Commun.* **2001**, 1890–1891; c) M. O. Vysotsky, O. Mogck, Y. Rudzevich, A. Shivanyuk, V. Böhmer, M. S. Brody, Y. L. Cho, D. M. Rudkevich, J. Rebek, Jr., *J. Org. Chem.* **2004**, *69*, 6115–6120.
[27] Each value is an average of two measurements see: D. J. Cram, H.-J. Choi, J. A. Bryant, C. B. Knobler, *J. Am. Chem. Soc.* **1992**, *114*, 7748–7765.
[28] P. S. Pregosin, E. Martínez-Viviente, P. G. A. Kumar, *Dalton Trans.* **2003**, 4007–4014.
[29] H. J. V. Tyrrell, K. R. Harris, *Diffusion in Liquids*, Butterworths, London, **1984**.
[30] P. A. S. Smith, G. F. Budde, S.-S. P. Chou, *J. Org. Chem.* **1985**, *50*, 2062–2066.

Received: January 10, 2005
Revised: June 1, 2005
Published online: September 27, 2005

